Catalysis Today xxx (2016) xxx–xxx

Contents lists available at ScienceDirect

Catalysis Today

journal homepage: www.elsevier.com/locate/cattod

Open cell foam catalysts for CO_2 methanation: Presentation of coating procedures and *in situ* exothermicity reaction study by infrared thermography

Myriam Frey[a], Thierry Romero[a], Anne-Cécile Roger[a], David Edouard[b,c,*]

[a] *ICPEES, UMR 7515, UMR 7515, Group "Energy and Fuels for a Sustainable Development", 25 rue Becquerel, 67087 Strasbourg, France*
[b] *USIAS (University of Strasbourg Institute for Advanced Study), Strasbourg, France*
[c] *LAGEP (Laboratoire d'Automatique et de Génie dEs Procédés), Université Claude Bernard Lyon 1, UMR CNRS 5007, 43 Bd du 11 Novembre 1918, 69622, Villeurbanne, France*

ARTICLE INFO

Article history:
Received 25 November 2015
Received in revised form 8 March 2016
Accepted 9 March 2016
Available online xxx

Keywords:
Coating
Platelet milli-reactors
Foam
CO_2 methanation
Infrared imaging
Heat capacity

ABSTRACT

The carbon dioxide methanation reaction is highly exothermal ($\Delta_R H = -165\ kJ\ mol^{-1}$). It is therefore essential to use processes able to control and efficiently evacuate the heat generated during the reaction. In this paper, a structured bed filled with an open cell foam was chosen due to the many advantages of this kind of reactor (high surface/volume ratio, low pressure drop, intensification of mass and heat transfer...). Three kind of open cell foams, with different thermal properties, were studied: SiC, Alumina and Aluminium. Coating procedures of a methanation catalyst (Ni/Ceria-Zirconia) developed in previous work for SiC open cell foams were adapted to alumina and aluminium open cell foams. For the first time, *in situ* infrared thermography was used to study the exothermicity of the reaction on the surface of different foams.

1. Introduction

Carbon dioxide is one of the gases responsible for the greenhouse gas effect. There are natural sources responsible for its presence (breathing, fermentation, fires, volcanoes, decomposition of organic matter...), but also anthropogenic ones (combustion of fossil resources and biomass, industries, agriculture...), the contribution of the last ones being massively and constantly increasing since the beginning of the industrial age. In order to reduce the CO_2 production or its emission into the atmosphere, many research projects about capture and storage emerged [1]. Another pathway to reduce these emissions is the valorisation of CO_2 by transforming it into valuable chemical compounds, like methane or longer hydrocarbon species, methanol, esters, ether... [2].

In Europe, most of the scenarios forecasting the energy mix by 2050 report an increase in the share of renewable energies (RE) at the cost of nuclear and fossil energies [3]. Solar and wind energies are intermittent and are hard to predict over the medium to long term. Furthermore, the energy production curves from RE are usually far away from the energy consumption curves. The energy produced needs to be stored. This storage can be of physical or chemical nature. Therefore, the "Power-to-Gas" (PtG) concept emerged as one of the chemical storage solutions. The aim of PtG (Fig. 1) is to use the excess of RE to produce first hydrogen through water electrolysis in order to inject the highest rate permitted directly into the already existing natural gas pipelines. The excess of hydrogen remaining and RE will then be converted into methane through carbon dioxide hydrogenation. The total amount of methane produced will also be injected into the natural gas pipelines. The PtG concept is a suitable way to contribute to the reduction or the stabilization of carbon dioxide in the atmosphere and to help modulating energy distribution.

The methanation reaction is highly exothermal ($\Delta_R H = -165\ kJ\ mol^{-1}$) and thermodynamically favored at low temperatures. It is therefore essential to have a process capable to efficiently evacuate the heat produced during the reaction in order to keep a constant reaction temperature (*e.g.* thermodynamically favorable). Moreover, an optimal temperature (*i.e.* without hot spot in the catalytic bed) allows to keep a proper selectivity and prevents a premature deactivation of the catalyst due to sintering. Among the processes actually used for this reaction, two types of reactors are used: fixed bed or fluidized bed. In the case of fixed

* Corresponding author.
E-mail address: david.edouard@univ-lyon1.fr (D. Edouard).

http://dx.doi.org/10.1016/j.cattod.2016.03.016
0920-5861/

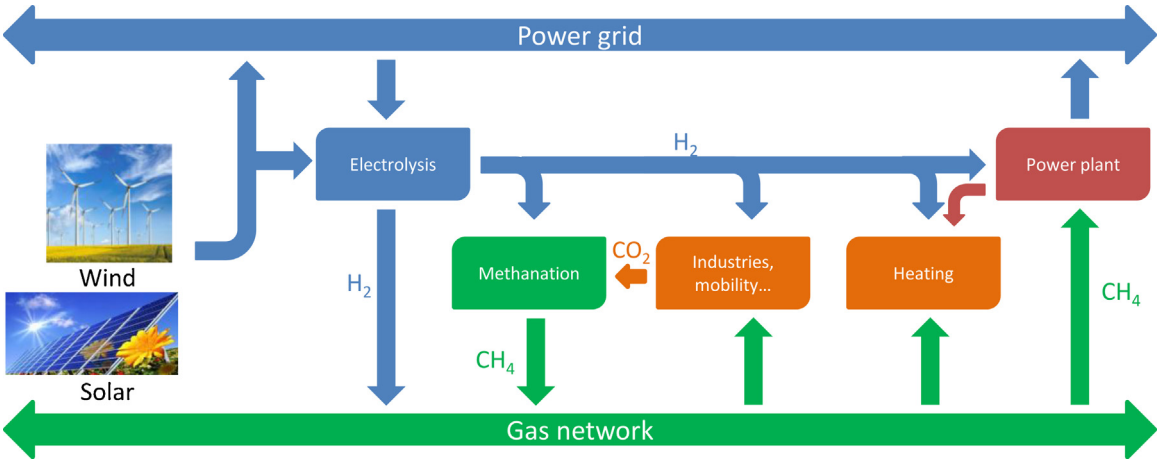

Fig. 1. Diagram illustrating the Power-to-Gas concept.

bed, the heat dissipation is poor and the only way to avoid thermal runaway is to work under a diluted reactant flow (and thus to limit the conversion rate). Fluidized bed allows efficient heat dissipation due to a high solid-fluid heat transfer coefficient. The counterpart of fluidized beds is that necessary to have continuous feeding of catalyst due to the attrition of the catalyst (resulting from as a result of continuous friction during fluidization). The catalyst becomes smaller, is carried away by the fluid and leaves the reactor, contaminating the downstream section of the process.

New processes combining the advantages of fixed and fluidized beds have been developed over the past years: structured beds (monoliths, static-mixer, fibrous networks, multi-channel beds. . .). Among these structured beds, those formed of open cell foams (OCF) coated with a catalyst offer many advantages: such as a high surface/volume ratio, low pressure drop, a better control of the reaction conditions, an intensification of mass and heat transfer [4–6]. The last one is very interesting for the intensification of the methanation reaction.

The objective of our work is to study the heat transfer of the highly exothermal carbon dioxide methanation reaction. In this study, a new platelet milli-reactor (PMR) is developed based on previous studies [7–11]. In order to study the heat transfer, an infrared camera is used. Therefore, the main modifications (compared to previous PMR [7–11], Fig. 2a) concern the heating system and the metallic host structure (*e.g.* an infrared window (ZnSe) is inserted in the upper part, Fig. 2b).

Most of the works published on heat study use thermocouples, restricting temperature measurements to a few local points. IR temperature measurement is commonly used for macro-scale heat transfer studies [12,13]. Only few papers over the past decade have been published for micro-scale heat studies; mainly single- and two-phase flow heat transfer studies [14]. In best of our knowledge, it is first time that a catalytic reaction in fixed bed is supervised, *in situ*, by thermal infrared camera.

The IR window used only stands a maximal temperature of 250 °C. Therefore, in previous work [15], preliminary studies were performed in order to choose a catalyst with enough catalytic activity (10–20% of CO_2 conversion) at temperatures below 250 °C. The catalyst chosen is composed of an active phase of nickel, often used in literature for CO_2 methanation [16–23], doped with ruthenium (molar ratio of Ni/Ru of 1:100), in order to lower the reduction temperature of the active phase [24,25], and a ceria-zirconia catalytic support [26]. The presence of ceria-zirconia was shown to be essential to achieve higher conversion rates and methane selectivity near 98–100%, which is probably due to its participation in the reaction mechanism as proposed by Ussa Aldana et al. [27].

In this paper, three OCF coated with a Ni-Ru/ceria-zirconia catalyst: silicon carbide (SiC), aluminium (Al) and alumina (Al_2O_3); with similar morphologies (*i.e.* approx. 30–40 PPI) but with different thermal properties (intrinsic conductivity) are used in order to show the effect of the heat transfer on the methanation reaction. First, we present the coating procedure (developed in previous

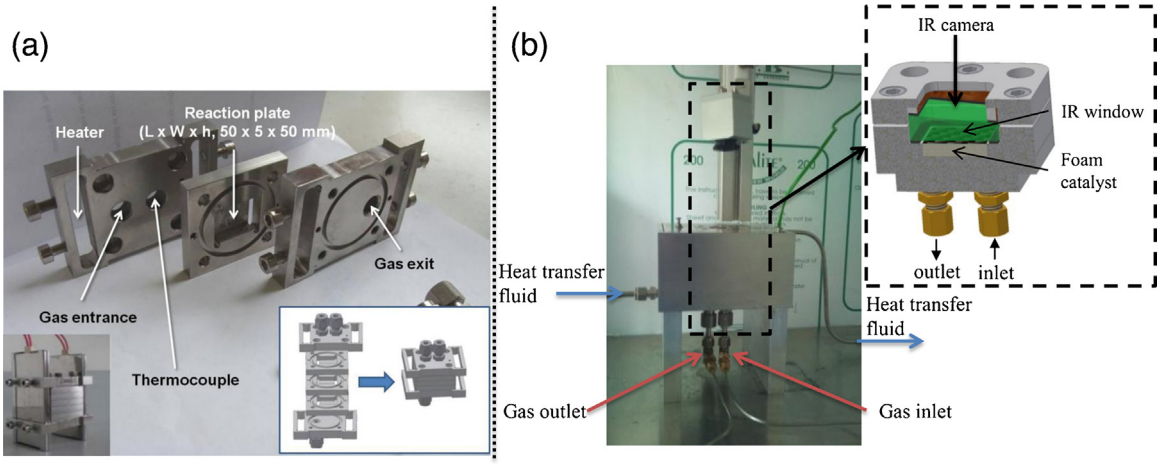

Fig. 2. Differences between the "conventional" (a) and new PMR used in for this study (b).

Please cite this article in press as: M. Frey, et al., Open cell foam catalysts for CO_2 methanation: Presentation of coating procedures and *in situ* exothermicity reaction study by infrared thermography, Catal. Today (2016), http://dx.doi.org/10.1016/j.cattod.2016.03.016

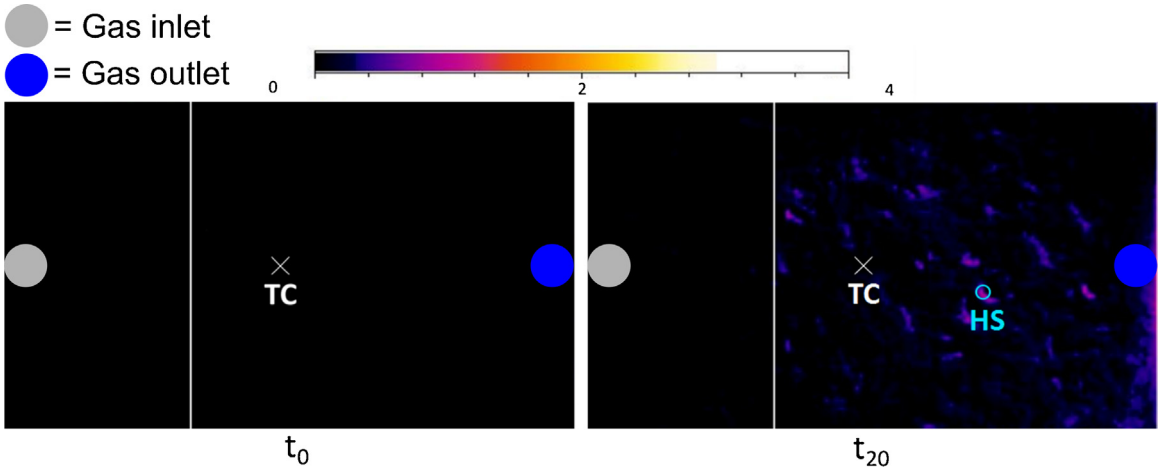

Fig. 3. Example of thermograph showing the position of uncoated OCF, coated OCF, thermocouple (TC) and hotspots (HS) at t = 0s (left) and t = 20s after the start of reaction (right).

work for SiC OCF) adapted for the aluminium and the alumina OCF. Then, for the first time, i*n situ* infrared thermography is used to monitor the heat generated on the catalyst surface during the methanation reaction. The aim of this study is to observe the hotspots formation for each OCF.

2. Material and methods

2.1. Preparation of the ceria-zirconia precursor solution

The ceria-zirconia precursor used was prepared by a « pseudo sol-gel » method [28]. The starting salts, cerium acetate (III) and zirconium acetylacetonate(IV), were dissolved separately in propionic acid (100 °C) in order to obtain a solution of 0.12 mol L^{-1} and generate the desired metallic propionates. Both solutions were then mixed and heated under reflux for 2 h in order to give mixed propionates. A distillation under progressive vacuum is performed to evaporate the solvent and leads, through oligomerization, to the formation of a resin. The resin is then dissolved in a given quantity of propionic acid to get the desired cationic concentration of precursor.

2.2. Foam coating procedure with ceria-zirconia

The foam is dipped for 10 min in the precursor solution. After removing the excess of solution under a nitrogen flow (2 bar), the foam is dried for 10 h and calcined under air at 500 °C for 6 h. Finally, the sample is placed in an ultrasound (US) bath for 10 min in order to remove the fraction of washcoat poorly anchored. An amount of 45 mg cm^{-3} of CZ was coated on each sample.

2.3. Foam impregnation of Ni-Ru

The samples were impregnated with nickel and ruthenium by dipping into an ethanolic solution of nickel nitrate hexahydrate and ruthenium acetylacetonate. The concentration of the solution is adapted to the amount of active phase desired per impregnation step. The foam is then dried at 100 °C for 2 h and calcined at 500 °C for 6 h under air. The SiC, Al_2O_3 and Al foams coated with CZ and impregnated Ni-Ru will be respectively named: SiC_{cat}, Al_2O_{3cat} and Al_{cat}. A total amount of 19 mg cm^{-3} of active phase is impregnated on each sample.

2.4. XRD characterization

X-ray diffraction patterns (XRD) were recorded on a Brüker D8 Advance diffractometer with a LynxEye detector side and Ni filtered Cu Kα radiation (1.5418 Å) over a 2θ range of 25–100 and a position sensitive detector using a step size of 0.012 and a step time of 0.5 s.

2.5. Infrared camera temperature calibration

In order to calibrate the temperature measured by the infrared camera (Optris PI 160: 160 × 120 Pixel and 120 Hz), an area above

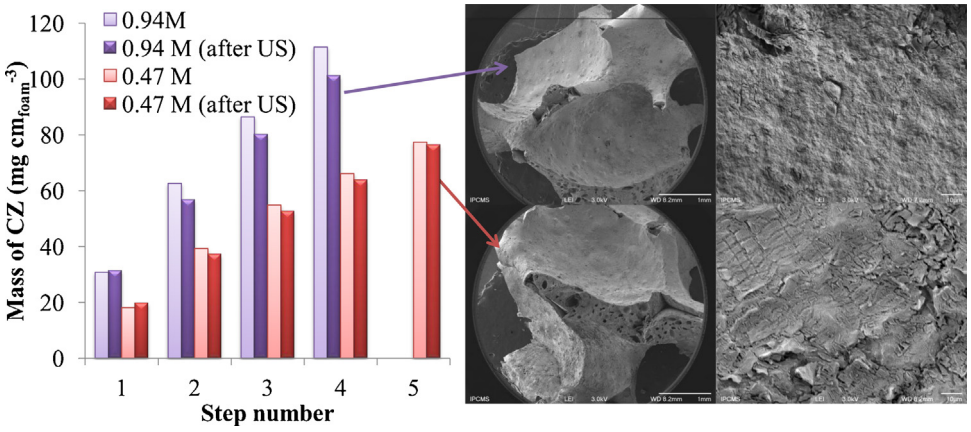

Fig. 4. Impact of the dipping solution concentration on the coating and anchoring efficiency of the washcoat.

Please cite this article in press as: M. Frey, et al., Open cell foam catalysts for CO_2 methanation: Presentation of coating procedures and *in situ* exothermicity reaction study by infrared thermography, Catal. Today (2016), http://dx.doi.org/10.1016/j.cattod.2016.03.016

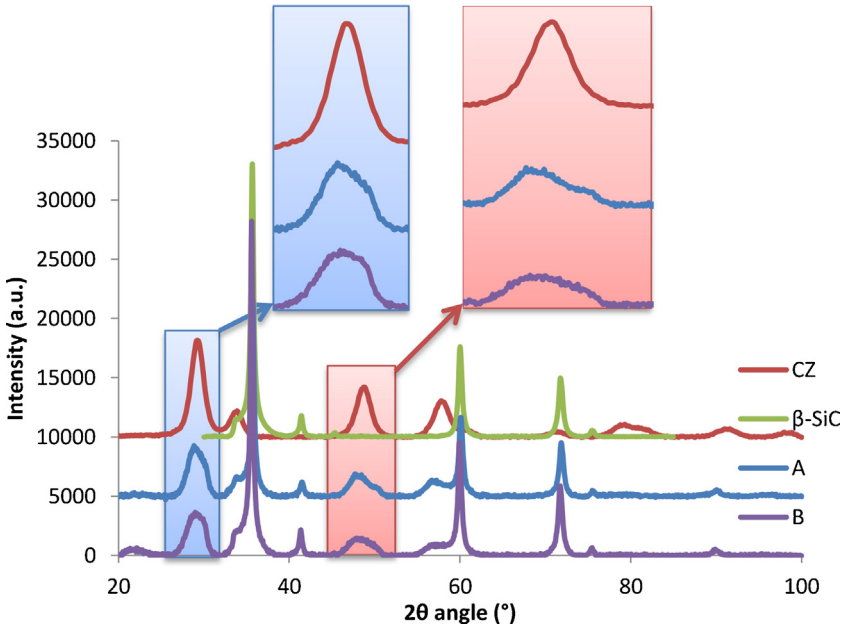

Fig. 5. XRD diffractograms of SiC coated with CZ (samples A and B), CZ and β-SiC.

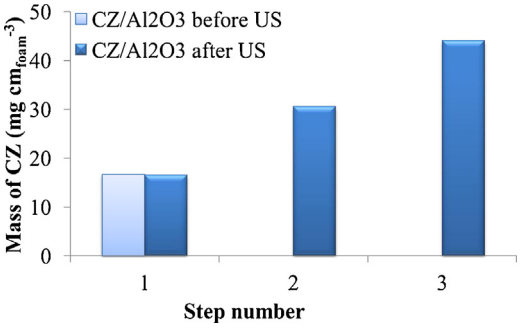

Fig. 6. Mass increase and anchoring of the washcoat on Al_2O_3 compared to SiC.

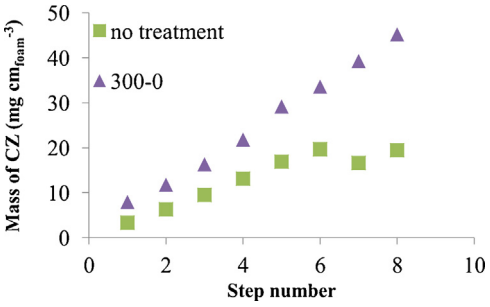

Fig. 8. Amount of washcoat deposited through eight coating steps after US.

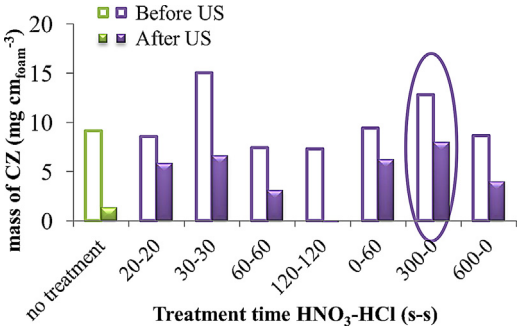

Fig. 7. Effect of the acidic treatment on the anchoring efficiency of the washcoat.

a thermocouple placed at the center of the reaction chamber was used. The calibration was performed under a flow of H_2/N_2 (molar ratio 36:10) with the same flow rate than used for the reaction. The calibration is performed by adjusting the emissivity value in order to have the same temperature value for this area and the corresponding thermocouple (Fig. 3). The deviation between the temperature measured with the thermocouple and the infrared camera is of ±0.5 °C. The emissivity values acquired are of 0.96 for SiC (literature: 0.83–0.96), 0.87 for Al_2O_3 (literature: 0.8) and 0.90 for Al (literature: 0.83–0.94) [29].

2.6. Test procedure

The reaction was recorded by an infrared camera positioned over the PMR through a ZnSe window. Two gas flows were used, 2 and 3 L h^{-1}, and the mass of catalyst per volume of reaction chamber was kept constant for the different foams studied. The reaction chamber was filled with two OCF: an uncoated foam at the gas inlet (OCF_{blank}), as a blank sample, filling 1/3 of the reaction chamber, followed by a foam coated with the catalyst (OCF_{cat}) filling the remaining 2/3 of the reaction chamber. The two foams where placed with a 1 mm gap between them in order to avoid any direct physical contact.

The catalyst was pre-reduced in an 80% H_2/N_2 stream (46 mL min^{-1}) in two steps. First in an external tubular reactor at 400 °C (heating rate: 2 °C min^{-1}) for 6 h, then inside the PMR (*i.e. in situ*) at 220 °C during 6 h to reduce the oxide layer that is formed during the transfer between reactors. The chamber temperature is increased (heating rate: 2 °C min^{-1}) to 220 °C under a flow of H_2/N_2 with a molar composition of 36:10 with the same flow rate than used for the reaction. The reactants are injected when the temperature inside the reactor chamber reaches a steady state. The reactant flow is composed of H_2/CO_2 (4:1), and N_2 as an internal standard. The molar ratio of $H_2/CO_2/N_2$ was 36:9:10. The feed and products were analyzed every 150 s using a programmable micro-chromatograph (Agilent M200H, TCD detector, alumina poraplot

Please cite this article in press as: M. Frey, et al., Open cell foam catalysts for CO_2 methanation: Presentation of coating procedures and *in situ* exothermicity reaction study by infrared thermography, Catal. Today (2016), http://dx.doi.org/10.1016/j.cattod.2016.03.016

Table 1
Catalytic test results, specific surface and heat flow produced during the reaction near of steady state (t = 2000s) for different OCF

OCF_{cat}	Flow rate ($L\,h^{-1}$)	X_{CO2} (%)	S_{CH4} (%)	S_{CO} (%)	S_{C2H6} (%)	S_{BET} ($m^2\,g^{-1}$)	Q (mW)
SiC_{cat}	2	7.8	94.3	4.1	1.6	33.8	45
	3	4.7	91.3	6.9	1.8		39
Al_2O_{3cat}	2	3.7	89.9	8.5	1.6	7.7	20
	3	2.3	84.7	14.0	1.4		18
Al_{cat}	2	2.3	83.0	14.8	2.2	6.3	11
	3	1.6	78.0	20.2	1.8		11

and molecular sieve 5 Å columns). The CO_2 conversion and CH_4 selectivity were defined as follows:

$$X_{CO_2}(\%) = \left(1 - \frac{A_{CO_2}}{A_{CO_2} + A_{CH_4} + A_{CO} + 2A_{C_2H_6}}\right) \times 10$$

$$S_{CH_4}(\%) = \left(\frac{A_{CH_4}}{A_{CO_2} + A_{CH_4} + A_{CO} + 2A_{C_2H_6}}\right) \times 100$$

X is the conversion, S the selectivity and A the surface areas of the peaks obtained by chromatography and corrected by their corresponding gas factors.

The theoretical heat flow (Q) generated during the reaction was estimated, using the conversion and selectivities defined above, by the following equation:

$$Q = F_{CH_4}\Delta_R H_{CH_4} + F_{CO}\Delta_R H_{CO}$$

Q_i is the heat produced by the generation of product i, F_i is the molar flow rate of product i and $\Delta_R H_{i,}$ is the enthalpy of reaction of product i.

The temperature rise of each pixel (ΔT_{pixel}, measured by the infrared camera) was calculated by the following relation:

$$\Delta T_{pixel}(t) = T_{pixel}(t) - T_{pixelatt<0}$$

$T_{pixel}(t)$ is the temperature measured by the infrared camera at time t and $T_{pixelat\ t<0}$ is the temperature measured by the infrared camera before the injection of the reactants (t < 0).

3. Results and discussion

3.1. Development of coating procedures

3.1.1. SiC foam

The β-SiC foam provided by SICAT has a low specific surface area ($S_{BET} \approx 25\,m^2\,g^{-1}$) that can be increased by calcination at 900 °C for 2 h under air. This thermal treatment procedure generates a natural SiO_2-SiOxCy wash-coat layer allowing a better anchoring of the active phase [15].

Two dipping solutions were prepared: a CZ precursor solution of 0.94 M in total cations (saturated solution) (sample A) and a 0.47 M solution prepared from the 0.94 M solution by dilution (sample B). The most concentrated solution will allow the lowest number of dipping steps to achieve a desired washcoat amount. The 0.47 M solution will allow us to study the impact of the dipping solution concentration on the anchoring strength of the washcoat. The washcoat amount deposited before and after ultrasounds (US) are presented Fig. 4. After the first coating, no loss of washcoat has been observed after US. The amount of washcoat remaining after US is respectively of 31.5 and 19.8 mg cm^{-3} of foam for A and B. After one coating step, the anchoring seems strong enough for both samples. After several coating steps, sample A shows a relative loss of 9% after each step, while the relative loss of sample B decreased from 5% to 1% over the coating steps. The anchoring is clearly stronger when a less concentrated solution is used. The SEM images (Fig. 4) show that the foam surface is completely covered regardless of the solution used. Sample A shows no cracking and a flat surface. Sample B shows an irregular surface with superficial craking, both certainly being responsible for the better anchoring of the washcoat.

XRD analysis were performed on the samples A and B (Fig. 5), β-SiC foam and CZ powder obtained by calcining a sample of the dipping solution. The XRD patterns of CZ powder show the presence of the fluorite cubic structure ($Ce_{0.4}Zr_{0.6}O_2$, JCPD card No. 00-038-1439), usually observed for ceria-zirconia mixed oxide with high contents of ceria [30,31]. Reflections corresponding to (111), (200), (220), (311), (222) and (400) planes are observed. The XRD patterns of uncoated β-SiC foam also show the presence of a fluorite cubic structure corresponding to β-SiC (β-SiC, JCPD card No. 00-001-1119). Reflections corresponding to (111), (200), (220), (311), (222) and (400) planes are observed. The SiC diffraction peaks remain at the same angle position after the coating of both samples compared to the uncoated β-SiC foam. In the case of CZ, the diffraction peaks belonging to the CZ crystallites of samples A and B show the presence of a shoulder at the left downside of the peaks at 2θ angle of 29° and 48° and the peaks after 79°, included, have disappeared or are under detection limit. These observations are suggesting crystalline phase segregation, indicating a chemical anchoring of the CZ washcoat on the foam.

3.1.2. Alumina foam

Most of the alumina foams commercially available are α-alumina ($S_{BET} \approx 1\,m^2\,g^{-1}$). The α phase is the most stable thermodynamically [32] among alumina phases, any thermal treatment would therefore be useless. The same coating procedure than for sample B was used on an alumina sample. The amount of washcoat deposited per coating step is presented Fig. 6. The amount of washcoat deposited per coating step shows a linear trend. After the first coating step, the amount of washcoat deposited was of 16.5 mg cm^{-3} with a relative loss of 0.8% under US. The amount of CZ deposited is similar to the SiC foam, as well as the quality of the anchoring. Therefore, despite the low surface area of the alu-

Table 2
CO_2 conversion values (X_{CO2}), ΔT_{mean} values, heat generated during the reaction (Q), sum of ΔT_{pixel} values and sum of ΔT_{pixel} values normalized by Q near of steady state (t = 2000s) for different OCF under same flow rate ($2\,L\,h^{-1}$)

Foam support	X_{CO2} (%)	ΔT_{mean} (K)	Q (mW)	$\sum_{i=0}^{n} \Delta T_i$ (K)	$\frac{\sum_{i=0}^{n} \Delta T_i}{Q}$ (K mW^{-1})
SiC_{cat}	7.8	0.94	45.4	4841	107
Al_2O_{3cat}	3.4	0.90	20.4	4629	227
Al_{cat}	2.3	0.37	11.4	1927	169

Please cite this article in press as: M. Frey, et al., Open cell foam catalysts for CO_2 methanation: Presentation of coating procedures and *in situ* exothermicity reaction study by infrared thermography, Catal. Today (2016), http://dx.doi.org/10.1016/j.cattod.2016.03.016

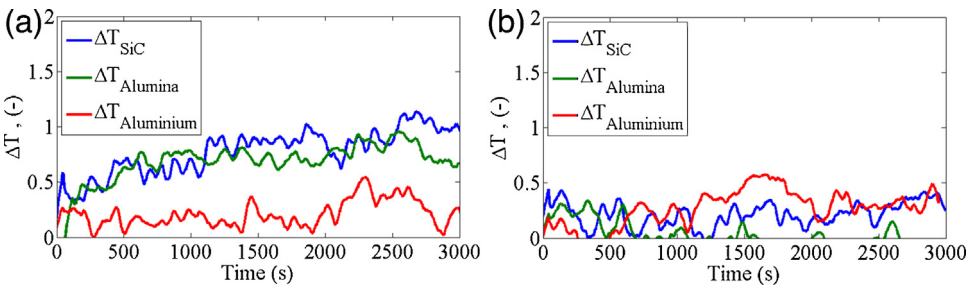

Fig. 9. ΔT_{mean} value of the foam samples over the time on stream under same flow rate (a: 2 L h^{-1} and b: 3 L h^{-1}).

mina foam, the strong anchoring is also probably due to a chemical anchoring, not to a physical one.

3.1.3. *Aluminium foam*

Aluminium foams have insignificant surface areas ($S_{BET} \approx 0.01$ m^2 g^{-1}). The coating procedures on metallic monolith reported in literature use acidic treatment with nitric acid or hydrochloric acid followed by nitric acid [33,34]. This kind of treatment is used on the one hand to dissolve a fraction of the natural alumina layer already coating the aluminium foam to create an uneven material surface and on the other hand to promote the development of a thicker alumina layer.

Fig. 7 displays the amount of washcoat deposited on the foam samples with the different acidic treatments tested. Without treatment 89% of the washcoat has been lost during the US. Short treatment of 20 s in chloric acid followed by nitric acid has lead to better anchoring with a relative loss of 32% after US and a washcoat of 5.8 mg cm^{-3}. An increase of the treatment time showed a negative effect on the anchoring with increasing relative losses after US from 56 to 100 %. The treatment that showed the highest wash-

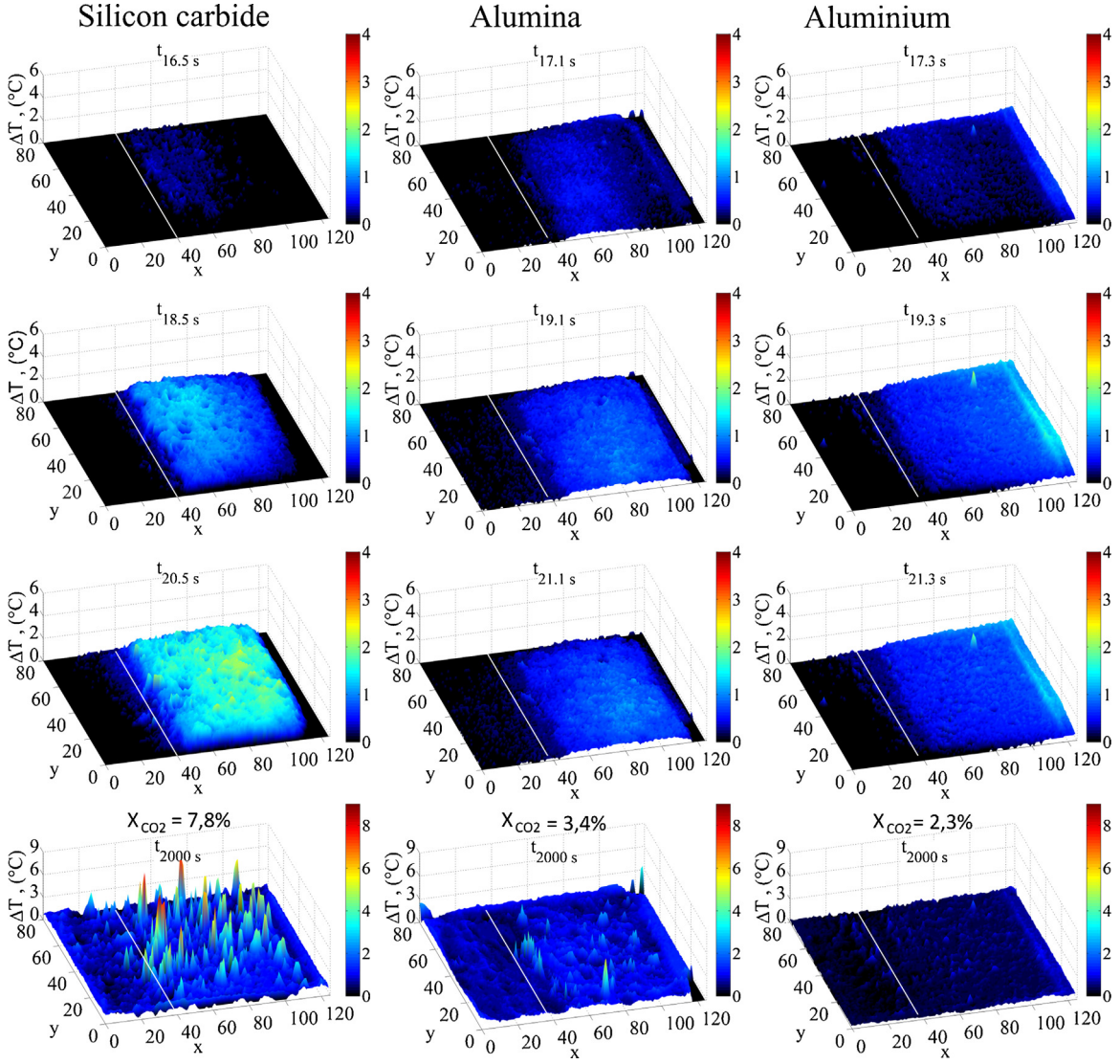

Fig. 10. ΔT mapping at the reaction ignition (t < 22s) and near of steady state (t = 2000s) for different OCF under same flow (2l/h).

Please cite this article in press as: M. Frey, et al., Open cell foam catalysts for CO_2 methanation: Presentation of coating procedures and *in situ* exothermicity reaction study by infrared thermography, Catal. Today (2016), http://dx.doi.org/10.1016/j.cattod.2016.03.016

coat deposition of 8.0 mg cm^{-3} and reasonable loss of 38% after US was achieved by dipping the foam in nitric acid for 300 s. Therefore, this chemical treatment procedure has been selected for aluminium foam coating.

Fig. 8 displays the mass of washcoat deposited per coating step depending on the chemical treatment chosen. The amount of coating per step increased linearly, achieving up to 45 mg cm^{-3} after 8 steps, unlike the untreated sample that showed an important loss of the washcoat after US at step 7 and achieving only a deposition of 19 mg cm^{-3} of washcoat after 8 steps.

In order to deposit the same amount of washcoat on the aluminium foam than the ceramic OCFs, twice the amount of coating steps have been required due to the lower anchoring strength.

3.2. Catalytic tests: infrared recording

3.2.1. Catalytic test results and heat production estimation

The CO_2 conversion values and selectivities of methane, carbon monoxide and ethane when the stationary state ($t \approx 2000s$) is reached during the catalytic tests are presented in Table 1. The CO_2 conversion rates of SiC_{cat}, Al_2O_{3cat} and Al_{cat} are respectively of 7.8, 3.7 and 2.3 for a flow rate of 2 L h^{-1} and 4.7, 2.3 and 1.6 for a flow rate of 3 L h^{-1}. The CO_2 conversion rates vary for the different OCF_{cats} although the catalyst loading is the same for every sample. These variations in terms of catalytic activity seem to be correlated with the specific surfaces (S_{BET}) of the OCF also given in Table 1. As reported in previous work [35], a lower specific surface will lead to a lower active phase particle dispersion and therefore to a smaller number of active sites and weaker catalytic activity. Regarding the selectivity values, it is important to remind that selectivities should be compared at isoconversion.

The results obtained for SiC_{cat} with a flow rate of 3 L h^{-1} and 2 L h^{-1} for Al_2O_{3cat} display selectivities of respectively 91.3 and 89.9% for methane and 6.9 and 8.5% for CO. The differences between these values are negligible regarding the difference in conversion (4.7 and 3.7% respectively) and analytical measurement error. The results at 3 L h^{-1} for Al_2O_{3cat} and 2 L h^{-1} for Al_{cat} can be directly compared, their conversion values are identical. Their selectivities are respectively of 84.7 and 83.0% for methane and 14.0 and 14.8% for CO.

3.2.2. Infrared camera temperature measurement during catalytic tests

The ΔT_{mean} value (the mean value of the ΔT_{pixel} inside the catalytic area), plotted *versus* the time for the different catalytic foams is shown Fig. 9. For each type of foam, the heat generated during the reaction, displayed in Table 1, is of the same order of magnitude for both flow rates studied. For the Al_2O_{3cat} sample for example, the heat generated are respectively of 20 and 18 under 2 and 3 L h^{-1}. However, the ΔT_{mean} values are clearly lower under a flow rate of 3 L h^{-1}. This result implies that the influence of the flow rate on heat evacuation cannot be neglected. Consequently, the comparison of the different type of foams can only be carried out under the same flow rate. Moreover, the differences between the different ΔT_{mean} (*i.e.* for different OCFs) are not obvious at 3 L h^{-1}. Therefore, in this work, we will only focus on the results of the catalytic tests performed under a flow rate of 2 L h^{-1}, because at 3 L h^{-1}, the influence of the flow rate is more important on the temperature profile at these conversion levels.

Thermographs representing the temperature rise for each pixel (as ΔT_{pixel} values), at the beginning of the reaction are displayed Fig. 10 for the different OCF studied. The OCF_{blank} sample doesn't show any temperature rise, whereas the OCF_{cat} clearly exhibits increasing temperature values. The beginning of the reaction was monitored and showed fast temperature increase, first at the entry of the OCF_{cat}, then the temperature increased all over the OCF_{cat} following the flow direction. The ignition time was of 4–5 s at 2 L h^{-1}.

Then, part of the heat generated by the reaction on the OCF_{cat} may be evacuated through the OCF_{blank}. Although there is no direct physical contact between OCF_{cat} and OCF_{blank}, they are indirectly linked by the bottom and side walls of the reaction chamber, which may explain the temperature increase on the OCF_{blank}.

Fig. 10 also displays a thermograph for each OCF_{cat} when a stationary state is reached (t = 2000s). SiC_{cat} which showed the highest catalytic activity also reveals the highest hotspots. Al_2O_{3cat} that exhibited lower catalytic activity than SiC_{cat} still shows some hotspots. For the Al_{cat}, it is difficult to confirm or refute clearly the presence of hotspots because the low conversion rate reached with Al_{cat} didn't produce enough heat.

In order to overcome the influence of the heat variation generated by the reaction (Q) for each OCF, we propose to normalize the sum of ΔT_{pixel} values by the corresponding Q value. The values displayed in Table 2 are respectively of 107, 227 and 169 K mW^{-1} for SiC_{cat}, Al_2O_{3cat} and Al_{cat}. SiC and Aluminium OCF show better results than alumina, which is coherent with intrinsic thermal conductivity values given in the literature (SiC = 4–5 W m^{-1} K^{-1} [36,37], Alumina = 1–2 W m^{-1} K^{-1} [35], Aluminium = 218 W m^{-1} K^{-1} [38,39]). SiC has theoretically a lower thermal conductivity than aluminium, however, the $\sum_{i=0}^{n} \frac{\Delta T_i}{Q}$ value of SiC_{cat} is lower than the one of Al_{cat}. From this work, the better performances are given by $SiC_{cat} > Al_{cat} > Al_2O_{3cat}$.

Two assumptions can be suggested to explain this result. First, because the conversion rates is low (in the case of Al_{cat}), the direct comparison is difficult.

Secondly, because the ceria-zirconia washcoat layer on the aluminium OCF is more important (compared to SiC), due to coating procedure (see for instance 3.1.3), it may have significant effect on the thermal conductivity properties of the Al_{cat}. The presence of this thicker oxide layer can locally decreases the thermal conductivity on the surface of the OCF. In addition, the chemical treatment performed on the aluminium OCF may also be affected the intrinsic thermal properties of the Al_{cat}

A complementary studies with samples which present similar textural properties, allowing same active phase dispersion (*i.e.* number of active sites), is essential to confirm or refute these assumptions.

4. Conclusion

In this work, the coating of a ceria-zirconia catalyst was optimized for three different open cell foams: silicon carbide, alumina and aluminium. SiC was thermally treated to increase its anchoring surface and a less concentrated dipping solution allowed better anchoring strength. The washcoat of untreated alumina showed the same anchoring strength than for SiC. Aluminium needed chemical treatment, but even with the best anchoring efficiency achievable, the washcoat showed a weaker anchoring than both ceramic open cell foams.

A heat transfer study was performed on these three catalytic foams. For the first time, the direct effect of the exothermal methanation reaction on the foam's surface temperature was recorded. This study allows to observe in-situ the ignition reaction and to show directly the formation of hotspots.

Further studies are necessary. It is important to increase the catalytic activity on metallic foam at 220 °C in order to achieve direct comparison of metallic and ceramic foams at isoconversion rates.

Acknowledgments

The authors would like to thank the ANR (project ANR2010JCJC90401 SIMI9 'Millimatrix'), the Région Alsace and

CNRS Emergence CO2 2014 (CAMICOM project) for their financial support.

References

[1] F. Lecomte, P. Broutin, E. Lebas, Le captage du CO_2, Editions Technip, Paris, 2010.
[2] J. Wambach, A. Baiker, A. Wokaun, Phys. Chem. Chem. Phys. 1 (1999) 5071–5080.
[3] COM(2011) 885 final. Commission des Communautés Européennes, Feuille de route pour l'énergie à l'horizon 2050, Bruxelles, (15.12.11).
[4] L. Giani, G. Groppi, E. Tronconi, Ind. Eng. Chem. Res. 44 (2005) 4993–5002.
[5] J.T. Richardson, D. Remue, J.K. Hung, Appl. Catal. A 250 (2003) 319–329.
[6] G. Hetsroni, M. Gurevich, R. Rozenblit, Int. J. Heat Mass Transf. 48 (2005) 3793–3803.
[7] S. Ivanova, E. Vanhaecke, S. Libs, B. Louis, C. Pham-Huu, M. Ledoux, patent n(: pct/fr2007/002017 (2008).
[8] Y. Liu, D. Edouard, L.D. Nguyen, D. Begin, P. Nguyen, C. Pham, C. Pham- Huu, Chem. Eng. J. 222 (2013) 265–273.
[9] Y. Liu, S. Podila, D.L. Nguyen, D. Edouard, P. Nguyen, C. Pham, M.J. Ledoux, C. Pham-Huu, Appl. Catal. A 409–410 (2011) 113–121.
[10] T.T. Nguyen, L. Burel, D.L. Nguyen, C. Pham-Huu, J.M. Millet, Appl. Catal. A 433 (2012) 41–48.
[11] M. Lacroix, L. Dreibine, B. de Tymowski, F. Vigneron, D. Edouard, D. Bégin, P. Nguyen, C. Pham, S. Savin-Poncet, F. Luck, M.J. Ledoux, C. Pham-Huu, Appl. Catal. A 397 (2013) 62–72.
[12] G.M. Carlomagno, L. de Luca, Handbook of Flow Visualization, Hemisphere Publishing Corporation, Washington, DC, 1989, pp. 531–553.
[13] B. Palm, Heat transfer in microchannels, Microscale Therm. Eng. 5 (2001) 155–175.
[14] G. Hetsroni, A. Mosyak, E. Pogrebnyak, R. Rozenblit, Int. J. Therm. Sci. 50 (2011) 853–868.
[15] M. Frey, D. Edouard, A.C. Roger, CR Chim. 18 (2015) 283–292.
[16] F. Ocampo, B. Louis, L. Kiwi-Minsker, A.-C. Roger, Appl. Catal. A Gen. 392 (2011) 36–44.
[17] C. Bartholomew, R.B. Pannell, J. Catal. 65 (1980) 390–401.
[18] A.E. Aksoylu, Z. Misirli, Z.I. Önsan, Appl. Catal. A Gen. 168 (1998) 385–397.
[19] F.-W. Chang, M.-S. Kuo, M.-T. Tsay, M.-C. Hsieh, Appl. Catal. A Gen. 247 (2003) 309–320.
[20] G. Zhi, X. Guo, Y. Wang, G. Jin, X. Guo, Catal. Commun. 16 (2011) 56–59.
[21] M. Cai, J. Wen, W. Chu, X. Cheng, Z. Li, J. Nat. Gas Chem. 20 (2011), 318–234.
[22] S. Tada, T. Shimizu, H. Kameyama, T. Haneda, R. Kikuchi, Int. J. Hydrogen Energy 37 (2012) 5527–5531.
[23] H. Song, J. Yang, J. Zhao, L. Chou, Chinese J. Catal. (Chinese Version) 31 (2010) 21–23.
[24] J.M. Rynkowski, T. Paryjczak, M. Lenik, Appl. Catal. A 126 (1995) 257–271.
[25] M. Wang, C.T. Au, S.-Y. Lai, Int. J. Hydrogen Energy 40 (2015) 13926–13935.
[26] M. Frey, G. Mignani, J. Jolly, A.C. Roger, Adv. Chem. Lett. 1 (2013) 257.
[27] P. Ussa Aldana, F. Ocampo, K. Kobl, B. Louis, F. Thibault-Starzyk, M. Daturi, P. Bazin, S. Thomas, A.C. Roger, Catal. Today 215 (2013) 201–207.
[28] J.L. Rehspringer, J.C. Bernier, Mater. Res. Soc. Symp. Proc. (2nd edn.) 72 (1986) 297–307.
[29] Basic Principles Of Non-contact. Temperature Measurement, IR basics Brochure-E2014–01-A), Optris GmbH, pp. 27–30.
[30] A.E. Nelson, K.H. Schulz, Appl. Surf. Sci. 210 (2003) 206–221.
[31] A. Kozlov, J. Catal. 209 (2002) 417–426.
[32] J.F. Shackelford, R.H. Doremus, Ceramic and glass materials: structure, in: Properties and Processing, Springer, New York, USA, 2008.
[33] A. Beauseigneur, I., Lachman, M., Patil, S., Swaroop, R. Wusirika, patent n(US5334570 A (1994).
[34] M. Valentini, G. Groppi, C. Cristiani, M. Levi, E. Tronconi, P. Forzatti, Catal. Today 69 (2001) 307–314.
[35] M. Frey, G. Mignani, J. Jolly, A.C. Roger, Adv. Chem. Lett. 1 (2013) 257–263.
[36] D. Edouard, T. Truong Huu, C. Pham Huu, F. Luck, D. Schweich, Int. J. Heat Mass Transf. 53 (2010) 3807–3816.
[37] R. Philippe, M. Lacroix, L. Dreibine, C. Pham-Huu, D. Edouard, S. Savin, F. Luck, D. Schweich, Catal. Today 147 (2009) 305–312.
[38] E. Bianchi, T. Heidig, C.G. Visconti, G. Groppi, H. Freund, E. Tronconi, Catal. Today 216 (2013) 121–134.
[39] E. Bianchi, T. Heidig, C.G. Visconti, G. Groppi, H. Freund, E. Tronconi, Chem. Eng. J. 198–199 (2012) 512–528.

Please cite this article in press as: M. Frey, et al., Open cell foam catalysts for CO_2 methanation: Presentation of coating procedures and *in situ* exothermicity reaction study by infrared thermography, Catal. Today (2016), http://dx.doi.org/10.1016/j.cattod.2016.03.016